Available online at www.sciencedirect.com
SCIENCE DIRECT®
Agricultural and Forest Meteorology 124 (2004) 15–29
AGRICULTURAL AND FOREST METEOROLOGY
www.elsevier.com/locate/agrformet

Measuring field-scale isotopic CO_2 fluxes with tunable diode laser absorption spectroscopy and micrometeorological techniques

T.J. Griffis [a,*], J.M. Baker [a,b], S.D. Sargent [c], B.D. Tanner [c], J. Zhang [a]

[a] *Department of Soil, Water, and Climate, University of Minnesota-Twin Cities, Borlaug Hall, 1991 Upper Buford Circle, St. Paul, MN 55108, USA*
[b] *USDA-ARS, St. Paul, MN 55108, USA*
[c] *Campbell Scientific, Inc., 815 West 1800 North, Logan, UT 84321-1784, USA*

Received 11 August 2003; received in revised form 29 January 2004; accepted 29 January 2004

Abstract

The combination of micrometeorological and stable isotope techniques offers a relatively new approach for elucidating ecosystem-scale processes. Here we combined a micrometeorological gradient technique with tunable diode laser absorption spectroscopy (TDLAS) using the Trace Gas Analyzer (TGA100, Campbell Scientific, Inc., Utah, USA) to measure field-scale isotopic CO_2 mixing ratios and fluxes of $^{12}CO_2$ and $^{13}CO_2$. The experiment was conducted in a recently harvested soybean (*Glycine max*) field that had been in corn (*Zea mays*) production the previous 4 years. Measurements were made over a period of 26 days from October 25 to November 19, 2002. Weather conditions were unusually cold and dry during the experiment. Isotopic gradients were small and averaged -0.153 and -0.0018 μmol mol^{-1} m^{-1} for $^{12}CO_2$ and $^{13}CO_2$, respectively for $u_* > 0.1$ m s^{-1}. The average $^{12}CO_2$ and $^{13}CO_2$ flux for the period was 1.0 and 0.012 μmol m^{-2} s^{-1}, respectively. The isotope ratio of respired carbon ($\delta^{13}C_R$) obtained from the linear intercept of a Keeling plot was -27.93‰ (± 0.32‰) for the experimental period. The Keeling plot technique was compared to a new flux ratio methodology that estimates $\delta^{13}C_R$ from the slope of a linear plot of $^{13}CO_2$ versus $^{12}CO_2$ flux. This method eliminates a number of potential limitations associated with the Keeling plot and provides a $\delta^{13}C_R$ value that can be directly related to the flux footprint. In this initial comparison, our analysis showed that the flux ratio method produced a similar $\delta^{13}C_R$ value (-28.67‰), but with greater uncertainty (± 2.1‰). Better results are expected during growing season conditions when fluxes are substantially larger and the signal to noise ratio is improved. The isotope ratio of respired carbon was consistent with C_3 agricultural systems indicating that soybean decomposition was the dominant substrate for respiration. The observed increase in ecosystem respiration (R_E) and decrease in $\delta^{13}C_R$ following tillage indicated that the incorporation of fresh soybean residue provided the major source for decomposition and further illustrates that the combination of micrometeorological and stable isotope techniques can be used to better interpret changes in carbon cycle processes. Long-term and continuous measurements of isotopic CO_2 exchange using tunable diode laser absorption spectroscopy and micrometeorological techniques offers a new opportunity to study carbon cycle processes at the field-scale.

Keywords: Tunable diode laser absorption spectroscopy (TDLAS); Micrometeorology; Stable isotopes; Keeling plot; Isotopic fluxes; Net ecosystem exchange; Ecosystem respiration

* Corresponding author. Tel.: +1-612-625-3117; fax: +1-612-625-2208.
E-mail address: tgriffis@umn.edu (T.J. Griffis).

0168-1923/$ – see front matter © 2004 Elsevier B.V. All rights reserved.
doi:10.1016/j.agrformet.2004.01.009

1. Introduction

The combination of micrometeorological and stable isotope techniques offers a relatively new approach for improving the description of ecosystem-scale processes (Yakir and Wang, 1996; Bowling et al., 1999, 2001). The stable isotopomers, $^{12}CO_2$ and $^{13}CO_2$, can be used as natural tracers to study biophysical processes because gross photosynthesis (P_g) discriminates against $^{13}CO_2$ and fixes proportionally more $^{12}CO_2$ (Farquhar et al., 1989). Consequently, the isotopic ratio of the atmospheric surface layer can become relatively enriched with $^{13}CO_2$ during the daytime. Lin and Ehleringer (1997) reported that on relatively short time-scales (<days), there was no significant evidence of discrimination caused by plant respiration. Recently, however, Duranceau et al. (1999) and Ghashghaie et al. (2001) demonstrated that respired CO_2 from the leaves of a variety of C_3 plants was enriched in $^{13}CO_2$ relative to the leaf metabolites. The amount of discrimination caused by dark respiration processes, however, is likely to be minor compared to that of P_g. Ecosystem respiration (R_E), therefore, adds relatively more $^{12}CO_2$ to the atmospheric surface layer causing it to become depleted in $^{13}CO_2$. The isotopic composition of respired carbon will differ from recently photosynthesized carbon because organic substrates, such as lignin and cellulose, exhibit differences in carbon isotope composition caused by enzymatic transformations following P_g (Ehleringer et al., 2000). The isotopic composition of R_E and P_g are not in equilibrium, which provides an opportunity to partition the net ecosystem CO_2 exchange (NEE) into its components using stable isotope techniques.

Differences in the relative isotopic abundance of ecosystem components can influence the isotopic signature of R_E, which can be used to help interpret changes in R_E (Lin and Ehleringer, 1997; Flanagan et al., 1999; Ehleringer et al., 2000). Furthermore, the distinct difference between C_3 and C_4 species in the degree of discrimination means that temporal changes in the isotope ratio of respired carbon can offer potential insight into the relative source contribution, mechanisms, and biophysical description of R_E in systems that have experienced known changes in species composition (Flanagan and Ehleringer, 1998; Ehleringer et al., 2002).

In recent years there has been increasing interest in the use of stable isotopes to study carbon cycling processes and to combine stable isotope and micrometeorological techniques to gain greater process information. There remains a need for obtaining continuous data at high temporal resolution to improve the understanding of land–atmosphere carbon cycling dynamics and ecosystem function. Previous experiments (Yakir and Wang, 1996; Bowling et al., 1999, 2001, 2003a) combined micrometeorological and stable isotope methods using flask sample air collection, stable isotope ratio analyses, and Keeling plots (Keeling, 1958) to estimate the isotopic fluxes of $^{13}CO_2$ and $^{12}CO_2$ and to characterize the isotopic signature of R_E. Bowling et al. (1999, 2001) used mass spectrometry with hyperbolic relaxed eddy accumulation (HREA) and the eddy covariance flask (isoflux) approach to measure isotopic fluxes. Flask measurement methods, however, are not well-suited to continuous and long-term monitoring of ecosystem exchange because they require significant amounts of manual field and laboratory labor. Furthermore, because flasks represent discrete, point-in-time samples, it is difficult to devise a measurement strategy that adequately captures all frequencies contributing to the flux. A new development in micrometeorology and trace gas research is the ability to measure $^{12}CO_2$ and $^{13}CO_2$ concentrations directly and continuously using tunable diode laser absorption spectroscopy (TDLAS). The Trace Gas Analyzer (TGA100, Campbell Scientific, Inc., Logan, UT) has recently been adapted to measure stable isotopomers (Bowling et al., 2003b). The relative high-frequency of isotopic CO_2 measurement using the TDLAS approach is unprecedented and the increase in temporal resolution should lead to greater insight into the biophysical controls on CO_2 exchange and ecosystem response to climate variation and land use practices. In particular, the TDLAS technique promises to provide better partitioning of NEE into P_g and R_E because a number of key parameters (isotope ratio of respiration and ecosystem discrimination) and quantities (isotopic fluxes) will be obtained at unprecedented frequency and duration. Thus, a better understanding of the diurnal, seasonal and interannual variations of these key parameters will be obtained.

This paper describes the results of a 26 day experiment where a micrometeorological gradient technique

and the TDLAS approach were combined to measure continuous $^{12}CO_2$ and $^{13}CO_2$ mole mixing ratios and fluxes over a recently harvested soybean field. The objectives of the paper were to:

1. Examine the variation in $^{12}CO_2$ and $^{13}CO_2$ mole mixing ratios and gradients related to atmospheric factors.
2. Estimate $^{12}CO_2$ and $^{13}CO_2$ fluxes using a gradient technique combined with eddy covariance estimates of eddy diffusivity.
3. Examine the variation in the isotope ratio of respired carbon.
4. Determine the suitability of the system for long-term and unattended measurements.

2. Methodology

2.1. Study site

Field research was conducted at the Rosemount Research and Outreach Center (RROC), University of Minnesota. RROC is located 20 km south of the St. Paul Campus (40°45′N, 93°05′W) at an elevation of 259.8 m.a.s.l. The experiment was conducted in a 17 ha agricultural field, which is relatively flat, homogeneous and with adequate fetch—at least 180 m in all directions. Peak flux footprint (x_{max}) (Schuepp et al., 1990) values obtained at the site are typically <40 m during unstable daytime conditions. The soil is a Waukegan silt loam (fine, mixed, mesic typic hapludoll), characterized by a surface layer of relatively high organic carbon content (2.6% average total organic carbon) and variable thickness (0.3–2.0 m) underlain by coarse outwash sand and gravel. The field was in corn (*Zea mays*, C_4 photosynthetic pathway) production for 4 years previous to the spring, 2002 planting of soybean (*Glycine max*, C_3 photosynthetic pathway). Depending on environmental conditions, the isotope ratio of C_4 plants has been shown to vary from −9 to −17‰ and C_3 plants −20 to −34‰ (Pate, 2001). The experiment began a few hours following soybean harvest on October 25 (day of year 298) and continued to November 19 (day of year 323). Prior to harvest the soybean canopy had completely senesced due to severe frost. Soybean harvest left plant residue on the soil surface but did not disturb the rooting system. Measurements were briefly interrupted on November 7 (day of year 311) while the field was tilled with a combination chisel plow/tandem disk.

2.2. Trace gas system

The stable isotopomers, $^{12}CO_2$ and $^{13}CO_2$, have unique absorption lines that can be selected and measured using the TGA (Bowling et al., 2003b). In order to measure an individual absorption line without overlapping other absorption lines the sample air pressure of the TGA was reduced to 2.0 kPa to reduce pressure broadening. $^{12}CO_2$ and $^{13}CO_2$ infrared absorption was measured at wavenumber frequencies of 2308.225 and 2308.171 cm^{-1}, respectively. A CO_2 reference gas with approximately 10% $^{12}CO_2$ and 0.1% $^{13}CO_2$ was maintained at a flow rate of 10 ml min^{-1} through the reference cell.

Mixing ratios of $^{12}CO_2$ and $^{13}CO_2$ were measured above the roughness sublayer at two sampling heights (1.65 and 2.35 m). Each sample inlet consisted of Delrin 25 mm filter holder with Teflon filter membranes (A-06623-32 and EW-02916-72, Cole-Parmer, Illinois, USA) followed by a brass critical flow orifice (Model D-7-BR, O'Keefe Controls Co., Monroe, CT, USA) to set a flow rate of 0.260 l min^{-1} and to maintain a TGA sample cell pressure of 2.0 kPa. Dekabon tubing (Dekabon Type 1300, 1/4 in. o.d. × 0.040 in. wall, Dekoron, Furon Brands, Aurora, Ohio, USA) connected the orifices to the inlets of desiccant cells (Gas Purifier A-01418-50, Cole-Parmer, Illinois, USA) filled with magnesium perchlorate. Dekabon tubing conducted the air streams back to the instrument trailer located at the edge of the field, a distance of approximately 200 m. The lag time for a sample entering the intake and reaching the TGA sample cell was 2 min and 14 s. Within the trailer, the two sample lines and two calibration gas lines were each connected through sample inlet valves (Model LHDA1223211HA, The Lee Co., Westbrook, CT, USA) mounted on a custom manifold (Campbell Scientific, Inc., Logan, UT, USA) to the TGA sample inlet. A rotary vane vacuum pump (RB0021, Busch, Inc., Virginia Beach, VA, USA) pulled the sample and calibration gases through the TGA sample cell. The manifold directed the flow from the unselected intakes (i.e. three of the four intakes) to the vacuum pump to maintain a constant flow in each intake.

This reduced pressure transients that could affect the measurements. Nitrogen gas, with flow rate of 10 ml min^{-1}, purged the sample detector housing and the air space between the laser and the sample cell to prevent absorption by ambient CO_2.

The TGA controlled the sampling system, with its parameters set to cycle through the four air streams every 2 min as follows: (1) calibration using ~350 μmol mol^{-1} CO_2 with known isotope ratio; (2) calibration using ~600 μmol mol^{-1} CO_2 with known isotope ratio; (3) measurement of CO_2 mixing ratio at height z_1; (4) measurement of CO_2 mixing ratio at height z_2. Within each 2 min cycle each calibration gas was sampled for 20 s, while each of the two measurement heights was sampled for 40 s. Following initial plumbing and leak testing, a zero gradient test was performed by moving both inlets to a common height, to ensure there were no systematic differences in the measured mixing ratios of the two sample lines.

The research trailer temperature was thermostatically controlled at approximately 20 °C to help maintain a stable calibration gain and offset. The TGA itself is enclosed in an insulated housing that is maintained at a constant temperature of approximately 35 °C. A two-point gain (G) and offset (O) correction, specific to each isotopomer, was performed every 2 min in order to obtain the $^{12}CO_2$ and $^{13}CO_2$ mixing ratios (see Bowling et al., 2003b for a detailed discussion of the gain and offset corrections).

2.3. Isotope convention, calibration standards and measurement precision

Our calibration procedure and data interpretation are referenced to the Vienna Peedee belemnite (VPDB) scale as recommended by the International Union of Pure and Applied Chemistry, Commission on Atomic Weights and Isotopic Abundances. The isotope relative abundance ($\delta^{13}CO_2$) of our standard gases and atmospheric samples were calculated from

$$\delta^{13}C = \left(\frac{R_s}{R_{VPDB}} - 1\right) \times 1000 \quad (1)$$

where R_s is the molar ratio of the heavy to light isotope ($^{13}C/^{12}C$) of the sample and R_{VPDB} the standard molar ratio ($^{13}C/^{12}C$). $\delta^{13}C$ is reported in parts per thousand (per mil or ‰).

The TGA calibration procedure requires that the mixing ratio of $^{13}CO_2$ and $^{12}CO_2$ be accurately known for the standard gases. Thus, the molar ratios of ^{13}C and ^{12}C in VPDB is required to determine the mixing ratio of $^{13}CO_2$ and $^{12}CO_2$ in each standard (see Appendix A for further details). We used R_{VPDB} to determine the mixing ratio of $^{12}CO_2$ and $^{13}CO_2$ in primary standards obtained from the National Oceanic and Atmospheric Administration-Climate Monitoring and Diagnostics Laboratory (NOAA-CMDL). The NOAA-CMDL standards were analyzed for total CO_2 mixing ratio and $\delta^{13}CO_2$ with values of 348.61 μmol mol^{-1}, −8.351‰ and 568.44 μmol mol^{-1}, −17.224‰, for cylinders A and B, respectively. Mole mixing ratios of $^{12}CO_2$ and $^{13}CO_2$ of the primary standards were calculated as 343.15, 3.80 and 559.60, 6.15 μmol mol^{-1} for cylinders A and B, respectively.

Secondary field standards were propagated by using the TGA to calibrate unknown calibration cylinders onsite. A detailed description of the field standards used during this experiment is provided in Table 1. During the period DOY 300 to DOY 318 we observed an increasing trend (~0.95% total CO_2 mixing ratio) in the standard cylinder B for $^{12}CO_2$ (calibration standard value 517.49 μmol mol^{-1}) and $^{13}CO_2$ (calibration standard value 5.72 μmol mol^{-1}) mixing ratios. No trend was observed in the corresponding standard cylinder A. The CMDL has reported the potential for trace gases to release from the walls of pressurized cylinders as cylinder pressure decreases (http://www.cmdl.noaa.gov/ccgg/refgases/airstandard.html). Consequently, the total CO_2 mixing ratio can increase with decreasing pressure (time). To correct this we detrended the drift in the $^{12}CO_2$ and $^{13}CO_2$ standard (cylinder B) prior to applying the two-point gain and offset corrections. This removed the trend that was introduced in the gain and offset factors. The variability and magnitude, however, were greater than expected during the period DOY 300 to DOY 318 as compared to the end of the experimental period when the secondary standards were changed.

The offset correction for each 2 min measurement cycle during the experimental period, shown in Fig. 1, averaged 2.97 (±1.42) and 0.039 (±0.015) μmol mol^{-1} for $^{12}CO_2$ and $^{13}CO_2$, respectively (the values in parenthesis indicate the standard deviation). The cor-

Table 1
Calibration standards and the uncorrected mixing ratio measurement of each standard used during the experimental period

DOY	Calibration standard values					
	Cylinder A			Cylinder B		
	$^{12}CO_2$	$^{13}CO_2$	$\delta^{13}CO_2$	$^{12}CO_2$	$^{13}CO_2$	$\delta^{13}CO_2$
[a]	343.15	3.80	−8.351	559.60	6.15	−17.224
298 (I)	348.87[b]	3.85	−13.546	517.49	5.72	−11.060
305 (II)	370.85	4.09	−14.411	517.49	5.72	−11.060
318 (III)	370.85	4.09	−14.411	584.32[b]	6.44	−13.632
	Uncorrected mixing ratio measurements of each standard					
	Cylinder A		Cylinder B			
	$^{12}CO_2$	$^{13}CO_2$	$^{12}CO_2$	$^{13}CO_2$		
298 (I)	345.42[b] (0.006)	3.81 (0.00004)	514.23 (0.02)	5.68 (0.0001)		
305 (II)	367.85 (0.007)	4.05 (0.00003)	514.35 (0.01)	5.68 (0.0001)		
318 (III)	367.38 (0.011)	4.05 (0.00006)	580.39 (0.02)[b]	6.40 (0.0001)		

[a] Indicates the NOAA-CMDL primary standards. The $^{12}CO_2$ and $^{13}CO_2$ mixing ratios were calculated for NOAA-CMDL standards based on the analyzed total CO_2 mixing ratio and $\delta^{13}CO_2$ values.

[b] Indicates original field standards. All other field standards were propagated from the original field standards. Mixing ratios are expressed in $\mu mol\,mol^{-1}$ and the isotopic ratio, $\delta^{13}CO_2$, in units of parts per thousand (‰). The values in parenthesis indicate the standard error of the mean. The uncorrected mixing ratios are the average measured values obtained over the time interval that each standard cylinder (A and B) was used during the experiment. I–III designate the time periods that these field standards were used as shown in Figs. 1 and 2. Note that the reported number of significant digits for the mixing ratios is inadequate to reproduce the $\delta^{13}CO_2$ values shown.

responding gain corrections were 1.000 (±0.0048) and 1.000 (±0.0041). Fig. 2 shows a significant reduction in the variability of the gain factor for DOY > 318 when the original cylinder B (calibration standard value 584.32 $\mu mol\,mol^{-1}$) was used for calibration. The mean and standard error of the uncorrected mixing ratios for the calibration standards (A and B) are shown in Table 1.

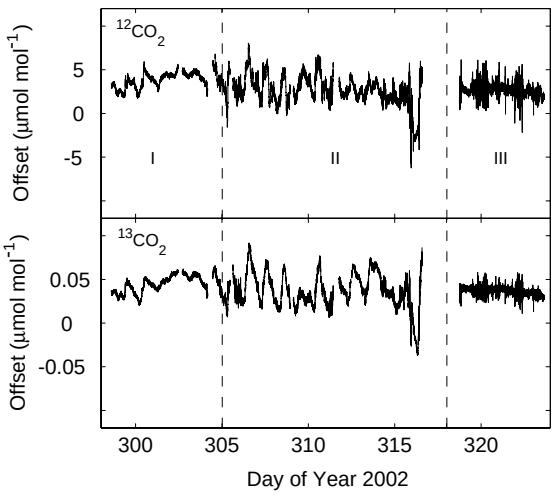

Fig. 1. Offset factors calculated for $^{12}CO_2$ (top panel) and $^{13}CO_2$ (bottom panel). The offset was calculated every 2 min using two known standard calibration cylinders. The time intervals I–III correspond to the calibration tank changes as described in Table 1.

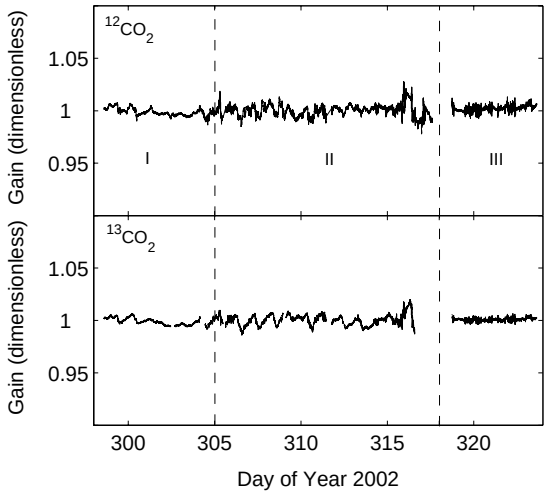

Fig. 2. Gain factors calculated for $^{12}CO_2$ (top panel) and $^{13}CO_2$ (lower panel). The gain was calculated every 2 min using two known standard calibration tanks. The time intervals I–III correspond to the calibration tank changes as described in Table 1.

The precision of the TGA was determined by measuring the $^{12}CO_2$ and $^{13}CO_2$ mixing ratios and the isotope ratio of two secondary standard cylinders for 34 half-hour periods. The mean and standard deviation of $^{12}CO_2$, $^{13}CO_2$ and $\delta^{13}CO_2$ for each cylinder was 348.87 ($\pm$0.03) μmol mol^{-1}, 3.8474 ($\pm$0.0002) μmol mol^{-1}, $-$13.55 ($\pm$0.07) ‰ and 584.32 ($\pm$0.05) μmol mol^{-1}, 6.4435 ($\pm$0.0005) μmol mol^{-1}, $-$13.63 ($\pm$0.03)‰, respectively.

2.4. Micrometeorological techniques

A three-dimensional sonic anemometer-thermometer (Model CSAT3, Campbell Scientific, Inc., UT, USA) was used to obtain the eddy diffusivity of the sensible heat flux (K). K was derived from

$$K = \frac{ku_*(z_2 - z_1)}{\phi} \quad (2)$$

where k is the von Karman constant, u_* the friction velocity, measured directly with the CSAT3, z_2 and z_1 are the measurement heights of the two air intakes and ϕ is the diabatic correction for atmospheric stability, calculated as described by Wagner-Riddle et al. (1996). Similarity was assumed for the diffusivity of sensible heat, CO_2, and its isotopomers.

Half-hour averaged flux calculations of net ecosystem CO_2 exchange (NEE) were computed from

$$\mathrm{NEE} = -K\frac{\bar{\rho}_a}{M_a}\frac{d\bar{X}}{dz} + \bar{\rho}_a\frac{d}{dt}\int_0^z \bar{X}(z)\,dz \quad (3)$$

where $\bar{\rho}_a$ is the density of dry air, M_a the molecular weight of dry air, and $d\bar{X}/dz$ the 30 min time-averaged vertical gradient of the CO_2 mixing ratio. The eddy flux is obtained from the first term on the right hand side of Eq. (3). The integral term is the rate of change in storage of CO_2 in the air column between the surface and the top of the CO_2 profile at height z_2. Corrections for density fluctuations resulting from sensible heat and latent heat fluxes (Webb et al., 1980) were eliminated because the air streams at each level were scrubbed of water vapor and brought to a common temperature at the analyzer.

Eddy covariance flux measurements of total CO_2 were obtained using the CSAT3 and an open-path infrared gas analyzer (LI-7500, LI-COR, NE, USA) measured at a height of 2 m. Post-processing of the data included 2-D coordinate rotation followed by simultaneous solution of the Webb et al. (1980) corrections and the Schotanus et al. (1983) equation, modified (Arjan van Dijk, pers. comm.) to account for the fact that the instantaneous sonic temperature measurements have already been corrected for cross-wind fluctuations, to determine the latent and sensible heat fluxes from the measured mean covariances of vertical wind speed with sonic temperature and with water vapor density. These were then used to compute a density-corrected CO_2 flux from the mean half-hour covariance of vertical wind speed and carbon dioxide concentration.

2.5. Keeling plot and flux ratio technique

The Keeling plot technique has been used extensively to characterize the isotope ratio of respiration ($\delta^{13}C_R$) at various spatial scales (Keeling, 1958; Buchmann and Ehleringer, 1998; Flanagan et al., 1999; Bowling et al., 2001; Pataki et al., 2003). Keeling (1958) demonstrated that there is a strong linear relationship between $\delta^{13}CO_2$ and the reciprocal of the total CO_2 mixing ratio. The decrease in $\delta^{13}CO_2$ with increasing CO_2 mixing ratio results from the addition of CO_2 to the atmosphere that has a different isotopic ratio than the background tropospheric value of approximately $-$8‰. In order to be linear, the added CO_2 to the atmosphere must have a constant isotopic ratio. If this is true the linear intercept of the Keeling plot can be used to quantify the isotope ratio of the added (respired) CO_2. We used this technique to examine the variability in $\delta^{13}C_R$ during this experiment. A geometric mean regression (Model II regression) method was used to estimate the Keeling intercept and slope (Pataki et al., 2003).

The uncertainty of the y-intercept for the Keeling plot technique remains an important issue (Yakir and Sternberg, 2000) because the linear equation must be extrapolated well beyond the range of the observed data. Furthermore, the intercept may be sensitive to changes in the background tropospheric isotope ratio, isotopic disequilibrium between daytime photosynthesis and nighttime respiration (Pataki et al., 2003) and changes in boundary layer depth and mixing (Lloyd et al., 1996). As shown in previous studies (Yakir and Wang, 1996; Bowling et al., 2001), the Keeling intercept provides one of the key parameters needed for partitioning NEE into R_E and P_g. One of the potential

advantages of the TDLAS technique is that, in contrast to the traditional Keeling plot approach, it allows a direct measurement of the isotopic fluxes. A flux ratio method, therefore, can be used to quantify the isotope ratio of R_E and can eliminate the potential problems mentioned above.

The traditional mass spectrometry technique fundamentally compares the isotopic ratio of a sample to the isotopic ratio of a reference material, leading to the use of the δ notation. The TDLAS technique, however, independently measures the mixing ratio of the two isotopomers. Although the δ notation is easily used (via Eq. (1)), a more direct approach is suggested: to determine the flux ratio of $^{13}CO_2$ to $^{12}CO_2$ as the slope of a linear fit. This ratio is then converted to the traditional δ notation. We obtained $\delta^{13}C_R$ from Eq. (1) as

$$^{13}CO_2 = \left(1 + \frac{\delta^{13}C_R}{1000}\right) \times R_{VPDB} \times {}^{12}CO_2 \quad (4a)$$

and taking the first-order derivative of $^{13}CO_2$ with respect to $^{12}CO_2$ yields

$$\frac{d^{13}CO_2}{d^{12}CO_2} = \left(1 + \frac{\delta^{13}C_R}{1000}\right) \times R_{VPDB} \quad (4b)$$

The term $d^{13}CO_2/d^{12}CO_2$ is obtained through the flux (gradient) measurement of $^{13}CO_2$ and $^{12}CO_2$. Therefore $\delta^{13}C_R$ can be defined as

$$\delta^{13}C_R = \left(\frac{F^{13}CO_2/F^{12}CO_2}{R_{VPDB}} - 1\right) \times 1000 \quad (4c)$$

where $F^{13}CO_2$ and $F^{12}CO_2$ are the isotopic effluxes—obtained during non-growing season or nighttime conditions. Application of this method during daytime growing season conditions would provide a flux ratio of NEE, which would include the effects of P_g and R_E. It should be noted that the source area influencing the flux ratio and the Keeling plot estimates of $\delta^{13}C_R$ are not equal. A concentration measured above the surface is associated with a larger source area than a flux measurement made at the same height (Schmid, 2002). Thus, the flux ratio method provides an estimate of $\delta^{13}C_R$ that can be related directly to the flux footprint.

3. Results

3.1. Climatic conditions

Conditions were unseasonably cloudy, cold, and dry during the measurement period. Fig. 3 shows the surface temperature measured with an infrared thermometer (Everest Interscience, Inc., AZ, USA) and cumulative precipitation recorded during the experiment. The average temperature for the period was 0.8 °C with an observed minimum and maximum of −10.6 and 18.1 °C, respectively. The warmest day coincided with the timing of tillage (DOY 311, November 7). Total cumulative precipitation during the experimental period was 3.4 mm. Approximately 3 mm of rainfall was recorded on DOY 308 (November 4). Conditions were extremely dry prior to the field experiment.

3.2. Variation in CO_2 mixing ratio and isotopic ratio

There was considerable variability in the mixing ratios of $^{12}CO_2$ and $^{13}CO_2$ (Fig. 4). The changes

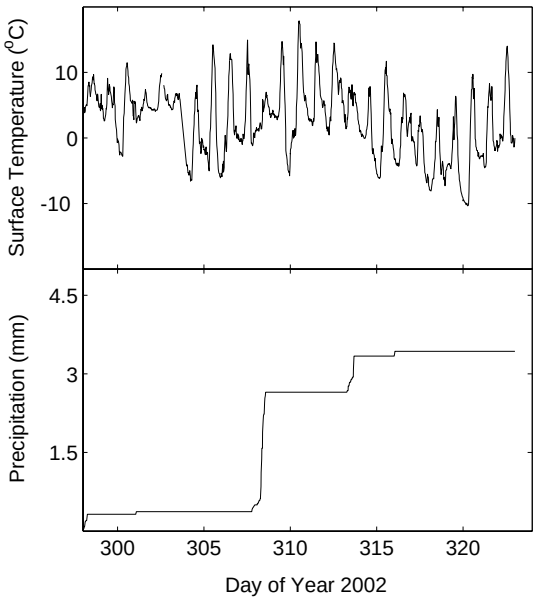

Fig. 3. Half-hour mean surface temperature measured with an infrared thermometer (top panel) and cumulative precipitation (bottom panel) measured during the course of the 26 day experiment. Climatic conditions were cloudy, and relatively cold and dry compared to the climate normal for Rosemount, Minnesota.

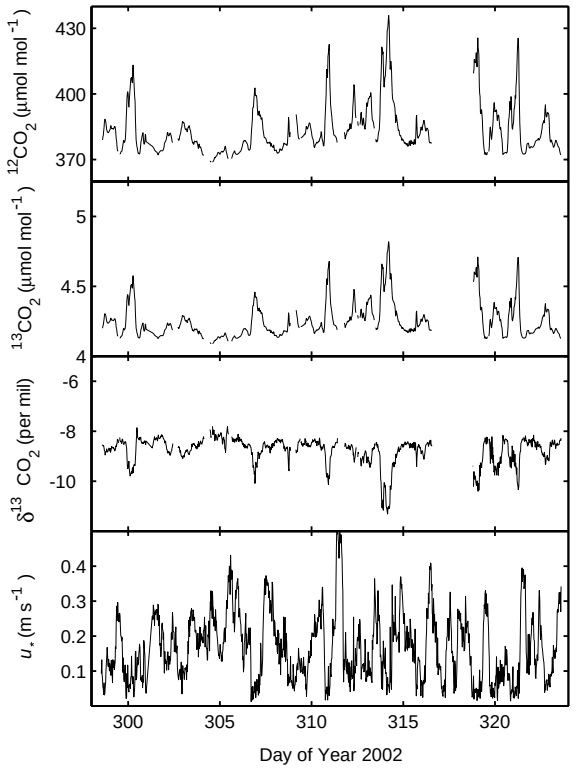

Fig. 4. $^{12}CO_2$ and $^{13}CO_2$ (top panels) mixing ratios, relative isotopic ratio ($\delta^{13}CO_2$) and friction velocity (u_*) (bottom panels). Large increases in $^{12}CO_2$ and $^{13}CO_2$ mixing ratios were observed for $u_* < 0.1\,m\,s^{-1}$. During these periods the isotopic ratio decreased as relatively $^{13}CO_2$ depleted carbon dioxide was respired into the nocturnal boundary layer. Measurements are shown for z_1 at 1.65 m.

in each isotopomer were highly correlated. Maximum values of $^{12}CO_2$ and $^{13}CO_2$ were 435.9 and 4.8 μmol mol^{-1}, respectively during the experimental period. The largest mixing ratios occurred on clear stable nights when u_* was less than $0.1\,m\,s^{-1}$ (weak turbulent mixing). The buildup of CO_2 during these stable conditions was relatively depleted in $^{13}CO_2$ resulting in a $\delta^{13}CO_2$ that was frequently less than −9‰. Fig. 5 illustrates the relation between total CO_2 and $\delta^{13}CO_2$ as a function of u_*. The strong increase in CO_2 and decrease in $\delta^{13}CO_2$ at u_* less than $0.15\,m\,s^{-1}$ reveals the effect of respired CO_2 accumulating in the developing nocturnal boundary layer. During prolonged stable atmospheric conditions the boundary layer $\delta^{13}CO_2$ was −11‰.

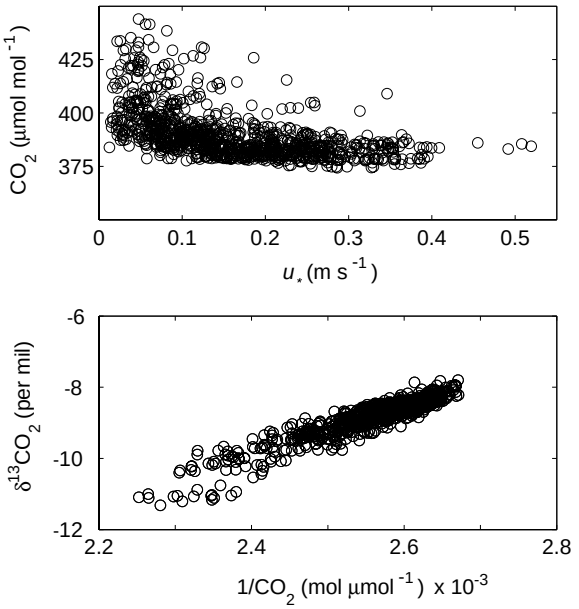

Fig. 5. Influence of friction velocity (u_*) on the total CO_2 mixing ratio and the relationship between total CO_2 mixing ratio and isotopic ratio ($\delta^{13}CO_2$) (Keeling plot). Each value represents a half-hour average. The amount of scatter shown in this Keeling plot illustrates the relatively large amount of variation observed over the course of this 26 day experiment. Measurements are shown for z_1 at 1.65 m.

3.3. Isotopic gradients and flux measurements

Gradients of $^{12}CO_2$ and $^{13}CO_2$ were relatively small during the measurement period. Mean gradients for $u_* > 0.1\,m\,s^{-1}$ were −0.153 and $-0.0018\,\mu mol\,mol^{-1}\,m^{-1}$, which was significantly larger than the precision of the measurement technique. Eddy covariance flux measurements of CO_2 and gradient flux measurements of $^{12}CO_2$ and $^{13}CO_2$ are shown for $u_* > 0.1\,m\,s^{-1}$ (Fig. 6). The fluxes were generally small due to the cold and dry conditions. A large increase in the CO_2, $^{12}CO_2$ and $^{13}CO_2$ flux was observed following tillage on DOY 311 and lasted about 3 days. This increase is consistent with the observations of others (Reicosky, 1997) and is probably attributable to the mixing of fresh surficial crop residue into the soil. This period also corresponded with relatively warm temperatures (Fig. 3). The average CO_2, $^{12}CO_2$ and $^{13}CO_2$ flux (for $u_* > 0.1\,m\,s^{-1}$) for the period was

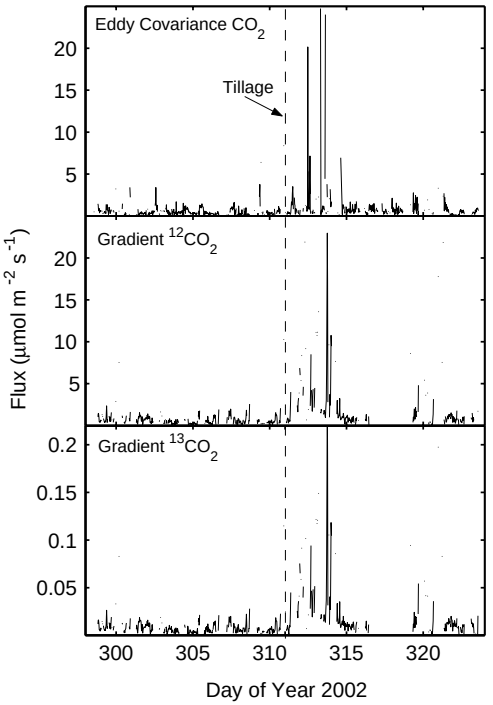

Fig. 6. Half-hour flux estimates of CO_2 (top panel), $^{12}CO_2$ (middle panel) and $^{13}CO_2$ (bottom panel). Total CO_2 fluxes were measured with a three-dimensional sonic anemometer and an open-path infrared gas analyzer. $^{12}CO_2$ and $^{13}CO_2$ fluxes were measured using the gradient technique. The largest fluxes were observed following tillage (DOY 311), which also correlated with relatively warm daytime temperatures.

0.80, 1.33, and 0.015 μmol m^{-2} s^{-1}, respectively. For $u_* > 0.15$ m s^{-1} the corresponding flux values were 0.84, 1.0 and 0.012 μmol m^{-2} s^{-1} illustrating that at low u_* the gradient technique overestimates the flux, presumably because gradient measurements are more sensitive to changes in storage. We also note that the eddy covariance flux measurements are likely underestimated because we did not correct for flux loss due to sensor separation or energy balance closure (Massman and Lee, 2002). The relative error of the gradient flux calculations was determined from the root mean squared error (RMSE) method (Bevington, 1969). Error propagation was estimated by examining the partial derivatives of the flux with respect to each of the dependent variables. We assumed a relative error of 15% for K and that the random error in measuring CO_2 mixing ratio vanishes with time. Furthermore, the systematic error between levels was assumed to be zero (zero gradient test) when calculating the finite differences in CO_2 mixing ratio (Griffis et al., 2000). The relative error propagating into the flux calculations was approximately 24% for $^{12}CO_2$ and $^{13}CO_2$.

3.4. Isotope ratio of ecosystem respiration

Fig. 7a shows the Keeling plot for all acceptable data ($u_* > 0.1$ m s^{-1}) collected during the experiment at measurement height z_1 (1.65 m). The $\delta^{13}C_R$ estimate (y-intercept of the linear equation) was −27.93‰ with a standard error of ±0.32‰ (Table 2). Similar results were obtained for height z_2 (2.35 m). The flux ratio $\delta^{13}C_R$ value was −28.67‰ with a standard error of ±2.1‰. Although the flux ratio technique avoids the extrapolation of the Keeling approach, it offered no real advantage in this particular experiment as the uncertainty in $\delta^{13}C_R$ was large compared to the Keeling method. We further explored the isotope ratio of respired carbon by examining the ratio of the change in storage (integral term of Eq. (3)), which is analogous to calculating a flux in an open-top-chamber. The $\delta^{13}C_R$ estimated from this approach was −27.76‰ with a standard error of ±0.62‰ (Fig. 7d). Finally, we calculated $\delta^{13}C_R$ using the ratio of $^{12}CO_2$ and $^{13}CO_2$ mixing ratios at each measurement height, which is fundamentally different than the flux ratio method. Although this method also avoids the problem of extrapolating to the y-intercept the $\delta^{13}C_R$ values were significantly less negative than the other approaches. There was generally good agreement between the Keeling plot and the flux ratio techniques.

The temporal variability of $\delta^{13}C_R$ (Fig. 8) was assessed by applying the Keeling plot and flux ratio method to two time intervals including pre-tillage (298 ≥ DOY ≥ 310) and post-tillage (311 ≥ DOY ≤ 323). Consistent with each approach was the strong decrease in $\delta^{13}C_R$ following tillage. Further analysis showed that the average surface temperature during the period of flux measurements was 3.8 °C prior to tillage and 1.0 °C following tillage. The decrease in $\delta^{13}C_R$, however, correlated with increased surface temperature and the large fluxes following tillage. Ideally, the isotope ratio of an individual half-hour efflux could be measured and used to assess the short-term variation in $\delta^{13}C_R$. However, given the small fluxes observed during the experimental period

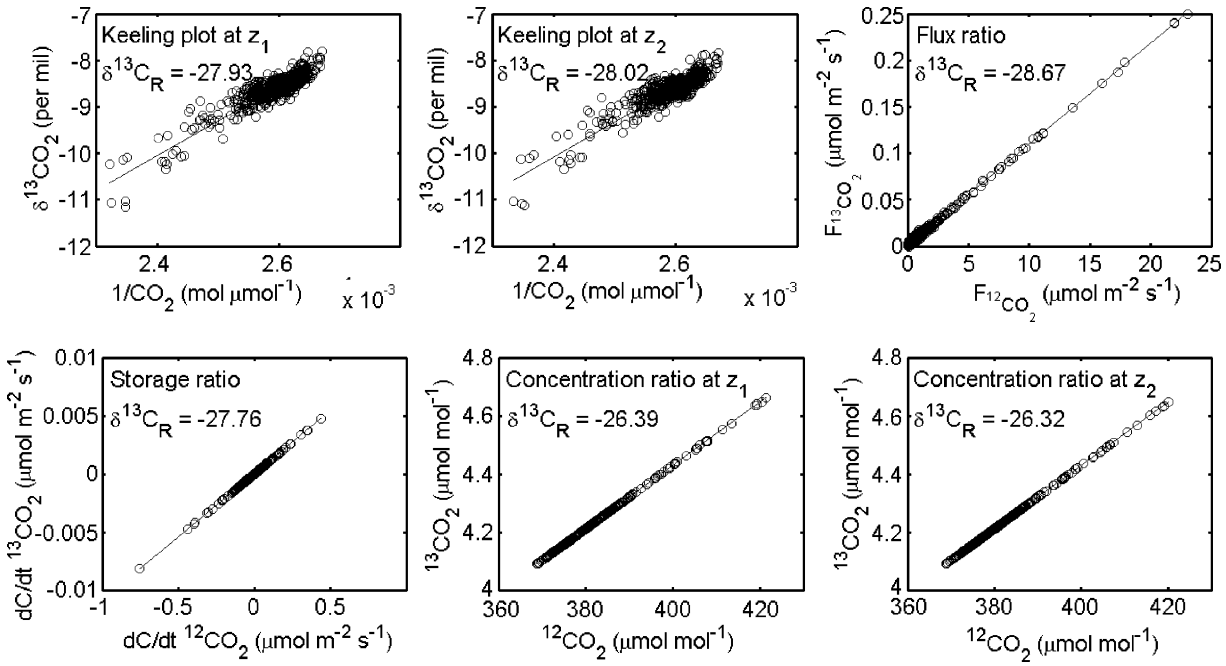

Fig. 7. Estimates of the isotopic ratio of respired carbon ($\delta^{13}C_R$) using the Keeling plot technique at height z_1 (top left panel) and z_2 (top middle panel) and alternative approaches using a linear plot of $^{13}CO_2$ vs. $^{12}CO_2$ flux (for friction velocity $> 0.1\,m\,s^{-1}$) (top right panel), storage ratio (bottom left panel), and mixing ratios at height z_1 (bottom middle panel) and height z_2 (bottom right panel). $\delta^{13}C_R$ was quantified using: (1) the intercept of the Keeling plot, (2) the slope of the linear plots (ratio technique). Each plot is based on coincident data in order to eliminate bias resulting from missing or screened values.

Table 2
Keeling plot and ratio techniques for estimating the isotopic signature of respired carbon at the field-scale

Technique	Slope	Intercept	$\delta^{13}C_R$	n	r^2 (adj)
Keeling plot (z_1)	7454	−27.93	−27.93 (±0.32)	656	0.83
Keeling plot (z_2)	7480	−28.02	−28.02 (±0.34)	656	0.81
Flux ratio	0.010859	0.001	−28.67 (±2.1)	656	0.99
Storage ratio	0.010869	−0.0000006	−27.76 (±0.62)	656	0.99
Conc. ratio (z_1)	0.010884	0.075	−26.39 (±0.30)	656	0.99
Conc. ratio (z_2)	0.010885	0.079	−26.32 (±0.31)	656	0.99

The comparative analysis was restricted to periods when data was available for each method (i.e. $n = 656$). Data were excluded for periods when friction velocity was $<0.1\,m\,s^{-1}$. Geometric mean regression was used for the fitting procedure. The values in parenthesis indicate the standard error of the parameter estimate.

the relative error in the flux ratio approach was significant. Daily estimates of $\delta^{13}C_R$ calculated from individual half-hour periods, for $^{12}CO_2$ flux $> 1.0\,\mu mol\,m^{-2}\,s^{-1}$, showed considerable variation over the course of the experimental period, with decreasing values associated with the large effluxes immediately following tillage. We could not conclude with certainty, however, that these daily variations in $\delta^{13}C_R$ were directly related to changes in biophysical factors.

4. Discussion

The combination of micrometeorological and stable isotope techniques offers the ability to gain additional

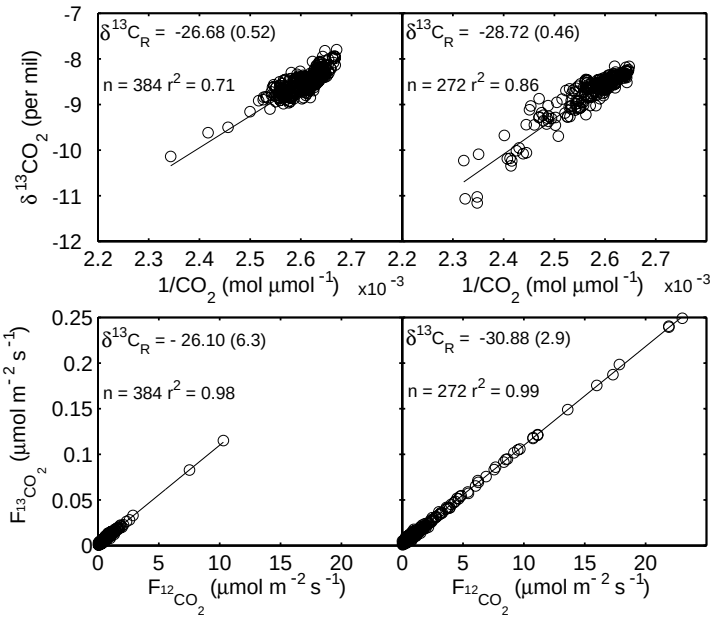

Fig. 8. Variability in the isotopic ratio of respired carbon ($\delta^{13}C_R$) using the Keeling plot technique (upper panels) and flux ratio method (lower panels). $\delta^{13}C_R$ was estimated for the time intervals including pre-tillage $298 \geq \text{DOY} \geq 310$ (left panels) and post-tillage $311 \geq \text{DOY} \geq 323$ (right panels). Each method showed that $\delta^{13}C_R$ became more negative following tillage. The values in parenthesis indicate the standard error of the parameter estimate.

process information at the field-scale. In the first study of its kind, Bowling et al. (2003b) compared in situ measurements using tunable diode laser absorption spectroscopy to laboratory analysis of flask samples using a stable isotope ratio mass spectrometer and an infrared gas analyzer. Their study showed that TDLAS concentration and isotopic ratio measurements compared well with the flask measurements, although they observed a systematic difference of 1.77‰, with the TDLAS technique underestimating (i.e. more positive) the $\delta^{13}CO_2$. They demonstrated that this offset was related to a pressure broadening effect caused by using calibration standards with CO_2 balanced in nitrogen rather than air. In this study we used TDLAS over a period of 26 days to measure mixing ratios of $^{12}CO_2$ and $^{13}CO_2$ at two heights to estimate isotopic fluxes from a recently harvested soybean field using the flux gradient method. Calibrations were performed with CO_2 balanced in dry air. The TGA system ran continuously during this period with data loss due only to system maintenance. Gradients of $^{12}CO_2$ and $^{13}CO_2$ were relatively small given the cold and dry weather conditions, but were larger than the limit of precision of the TGA system. The prospect of applying this approach for continuous year-long measurements shows considerable promise.

Consistent with flask-based measurement studies was an observed buildup of CO_2 in the nocturnal boundary layer that was relatively depleted in $^{13}CO_2$ due to the contribution of respiration (Bowling et al., 1999, 2001). For stable atmospheric conditions, $z/L > 0$ and $u_* < 0.1\,\text{m}\,\text{s}^{-1}$, the maximum total CO_2 mixing ratio exceeded $430\,\mu\text{mol}\,\text{mol}^{-1}$ with a $\delta^{13}CO_2$ of -11‰. This amount of depletion is consistent with nocturnal and early morning observations made by Bowling et al. (1999, 2001) for a deciduous Tennessee forest. The temporal variation in $\delta^{13}CO_2$ showed a consistent pattern of depletion on stable nights and a return to the daytime well-mixed $\delta^{13}CO_2$ value of approximately -8‰. Isotopic fluxes of CO_2 were small over the majority of the study period. In general, total flux estimates from the gradient approach ($^{12}CO_2 + {}^{13}CO_2$) were larger than the eddy covariance estimates. However, eddy covariance and the gradient fluxes showed a strong temporal correlation with the largest fluxes observed following tillage on day of year

311 (November 7). Large post-tillage fluxes were persistent for approximately 3 days, which corresponded with relatively warm days during the experimental period.

We estimated $\delta^{13}C_R$ to be −27.93‰ using the Keeling plot technique for the entire experimental period. The Keeling plot technique was compared to a new flux ratio method, which in theory, is less sensitive to changes in background atmospheric CO_2 mixing ratios and $\delta^{13}CO_2$ related to boundary layer dynamics (growth and entrainment), eliminates the problem of extrapolating to the *y*-intercept, and provides a $\delta^{13}C_R$ value that is consistent with the source area of the flux. The flux ratio estimate of $\delta^{13}C_R$ is based on the slope of a linear geometric mean regression fit. Thus, it eliminates the problem of projecting to the *y*-axis (i.e. 1/infinite CO_2 concentration), which is well beyond the range of the observed data. This approach produced $\delta^{13}C_R$ values that were more negative (∼0.7‰) than the Keeling approach; however, the uncertainty was large (>2‰) because the fluxes were very small. Better results are expected during growing season conditions when fluxes are significantly larger and the signal to noise ratio is improved. In this first attempt we find that the relatively small difference between the flux ratio and Keeling plot $\delta^{13}C_R$ values indicates that the Keeling method is very robust despite the potential uncertainty related to projecting to the *y*-intercept and beyond the range of observed data. Furthermore, it is relatively easier to measure than fluxes. Thus, continuous isotopic mixing ratio measurements using TDLAS with traditional eddy covariance flux measurements will offer new information for studying carbon cycle dynamics and ecosystem function.

Contrary to our original expectation, the isotopic ratio of respired carbon did not consistently become heavier (less negative $\delta^{13}C_R$) with time due to a reduction in fresh soybean residue relative to the 4-year accumulation of corn residue. We found $\delta^{13}C_R$ values that were consistent with C_3 agricultural systems (Ehleringer et al., 2000) indicating that soybean decomposition dominated respiration. Most intriguing was the change in $\delta^{13}C_R$ following tillage, which correlated with a short-term increase in temperature. We hypothesize that these changes resulted from: (1) incorporation of surface soybean residue and increased microbial decomposition following tillage on DOY 311, (2) an increase in microbial activity in response to warmer surface temperatures. The analysis illustrates that soybean (C_3) substrates were the main source for microbial decomposition following tillage despite the previous 4 years of corn production. Long-term continuous data are needed to further examine the influence of soil temperature, soil water content, and soil disturbance on the temporal variability $\delta^{13}C_R$ and the fluxes of $^{12}CO_2$ and $^{13}CO_2$. Estimating the contribution of fresh versus old carbon to R_E will be possible by combining atmospheric isotopic measurements with stable isotope plant and soil assays.

The high-frequency measurement of isotopic ratios and fluxes has the potential to offer considerable insight into the controls on R_E. Temporal variation in $\delta^{13}C_R$ suggests changes in the source contribution of respired carbon. Such changes probably reflect isotopic differences in organic matter and differential rates of microbial activity related to changes in temperature, water availability and disturbance of the soil profile. During growing season conditions, when fluxes are relatively large, we expect that the isotope ratio of R_E (at night) and NEE (daytime) could be obtained with a relatively small error on an individual half-hour basis using the flux ratio method.

Quantifying the temporal variability in $\delta^{13}C_R$ has major implications for flux partitioning studies (Yakir and Wang, 1996; Bowling et al., 2001). If the flux ratio of respiration is conservative on diurnal time-scales (>1 day) then the direct partitioning of daytime NEE into P_g and R_E should be possible from daytime flux measurements of $^{12}CO_2$ and $^{13}CO_2$ and estimates of ecosystem discrimination. Continuous long-term measurements of isotopic CO_2 exchange are needed to help partition NEE into its components and to better understand the temporal variability of $\delta^{13}C_R$ and photosynthetic discrimination. Such studies should make a valuable contribution to the regional carbon modeling community (Ciais et al., 1995; Francey et al., 1995; Fung et al., 1997).

5. Conclusions

1. Long-term and relatively high-frequency measurements of isotopic CO_2 mixing ratios and fluxes are possible using tunable diode laser absorption spectroscopy.

2. Eddy covariance flux measurements of total CO_2 and gradient flux measurements of $^{12}CO_2$ and $^{13}CO_2$ measured using the TGA system showed a strong temporal correlation.
3. Linear plots of $^{13}CO_2$ versus $^{12}CO_2$ fluxes support the Keeling plot technique for estimating the isotope ratio of respired carbon ($\delta^{13}C_R$) and provide a more direct means of evaluating the variation in the isotope ratio of ecosystem respiration.
4. The observed increase in ecosystem respiration (R_E) and decrease in $\delta^{13}C_R$ following tillage indicated that the incorporation of fresh soybean residue provided the major source for decomposition and further illustrates how combining micrometeorological and stable isotope techniques can be used to better interpret changes in carbon cycle processes.

Acknowledgements

Funding for this research was provided by the University of Minnesota, Grant-in-Aid-of-Research, Artistry and Scholarship Program (TJG). Field assistance was provided by W.A. Breiter and K. Vang, USDA-ARS Technicians, University of Minnesota. We gratefully acknowledge the logistical support provided by the Rosemount Research and Outreach Center, University of Minnesota and the USDA-ARS. We thank T.A. Black and K. Morgenstern for reviewing an earlier draft of the manuscript. We especially acknowledge the criticisms and helpful suggestions provided by D.R. Bowling and the anonymous reviewers.

Appendix A. Isotope standards and calculation of isotopomer mixing ratios

Most isotope ratio measurements are made with mass spectrometers and the results are reported as a relative difference in the isotope ratio compared to a standard ratio. Calculations are normally performed using delta notation, avoiding the use of the actual value for the standard ratio. The TGA100 fundamentally measures the mixing ratio of individual isotopomers—not their ratio. Therefore we report some results as mixing ratios and fluxes of individual isotopomers. Where appropriate, we also report our results in the familiar delta notation. In this appendix we present our methods for converting into and out of delta notation and discuss the origin of the constants used for these conversions.

Total mixing ratios and isotope ratios are calculated from the mixing ratios of individual isotopomers using Eqs. (A.1) and (A.2):

$$[CO_2] = \frac{[^{12}CO_2] + [^{13}CO_2]}{1 - f_{other}} \quad (A.1)$$

$$\delta^{13}C = 1000 \times \left(\frac{[^{13}CO_2]/[^{12}CO_2]}{R_{VPDB}} - 1 \right) \quad (A.2)$$

Eqs. (A.1) and (A.2) are rearranged to calculate the mixing ratios of individual isotopomers from the total mixing ratio and the isotope ratio:

$$[^{12}CO_2] = \frac{[CO_2](1 - f_{other})}{1 + R_{VPDB}(1 + \delta^{13}C/1000)} \quad (A.3)$$

$$[^{13}CO_2] = [CO_2](1 - f_{other}) - [^{12}CO_2] \quad (A.4)$$

where f_{other} is the fraction of CO_2 containing all isotopomers other than $^{12}C^{16}O^{16}O$ and $^{13}C^{16}O^{16}O$ (predominantly $^{12}C^{18}O^{16}O$ and $^{12}C^{17}O^{16}O$). We assume $f_{other} = 0.00474$, from the isotopic abundances used for the high-resolution transmission molecular absorption database (HITRAN), based on the work of De Bièvre et al. (1984).

Isotope ratios are reported relative to the Vienna Peedee belemnite scale, which is defined by assigning a value of 1.95‰ to the National Institute of Standards and Technology (NIST) reference material (RM) 8544 (NBS19) (Coplen, 1994, 1995). The NIST Report of Investigation for RM8544 gives the carbon isotopic abundance as 98.8922 atom percent ^{12}C and 1.1078 atom percent ^{13}C (NIST Report of Investigation from Reed, 1992), citing the measurements of Zhang and Li (1990). Zhang and Li measured the isotopic abundance of ^{13}C in NBS19 with mass spectrometers calibrated with CO_2 produced from mixtures of nearly pure $Ba^{12}CO_3$ and $Ba^{13}CO_3$, reporting a value for $R_{13,NBS19} = 11201.5 \times 10^{-6} \pm 4.5 \times 10^{-6}$. Zhang and Li calculated a total uncertainty of 28×10^{-6}, rounded $R_{13,NBS19}$ to 0.011202, and then converted it to the atom percentages included in the NIST report. To avoid accumulated round-off errors, we base our value of the reference ratio R_{VPDB} on the original measurement of Zhang and Li where $R_{VPDB} =$

0.0112015/1.00195 = 0.0111797. Considering the uncertainty reported by Zhang and Li (28×10^{-6}), this result should be rounded to 0.01118, but given the measurement precision of mass spectrometers (and tunable diode laser spectrometers) we arbitrarily retain the extra digits.

Our value for R_{VPDB} differs from the commonly cited value for $R_{PDB\text{-}Chicago}$, 0.112372, reported by Craig (1957) by approximately 5‰. Craig's value is based on the work of Nier (1950), who measured the isotopic abundance of ^{13}C in Solenhofen limestone using mass spectrometers calibrated with prepared mixtures of nearly pure ^{36}Ar and ^{40}Ar. Craig made a small correction to the value reported by Nier, and measured a sample of Nier's Solenhofen limestone relative to his own PDB limestone to arrive at the Craig value for $R_{PDB\text{-}Chicago}$. Zhang and Li (1990) noted the discrepancy between their measurement and the work of Craig and Nier, suggesting a bias in Nier's measurements caused by calibrating the mass spectrometer with argon isotopes (with mass 36 and 40) rather than CO_2 isotopomers (with mass 44 and 45).

In our terminology, we differentiate the VPDB standard ratio, R_{VPDB}, from the ratio reported by Craig, $R_{PDB\text{-}Chicago}$, which refers to the sample of Cretaceous Belemnite from the Peedee formation of South Carolina that was used as a calibration standard at the Enrico Fermi Institute for Nuclear Studies at the University of Chicago. This sample was exhausted many years ago, but comparisons made between various reference materials (for example, Craig (1957) and Coplen et al. (1983)) allowed the current standard to be defined with respect to an available reference material, NBS19, while maintaining approximate continuity with previous work referred to the PDB-Chicago standard.

Craig gives the equation by which measurements made with one standard (designated as *B*) may be reported relative to another standard (PDB):

$$\delta_{(x-\mathrm{PDB})} = \delta_{(x-B)} + \delta_{(B-\mathrm{PDB})} + 10^{-3}\delta_{(x-B)}\delta_{(B-\mathrm{PDB})} \quad \text{(A.5)}$$

This illustrates how measurements may be made using a working standard and reported with respect to the VPDB standard, which does not physically exist as a reference material. Measurements can be made using NIST RM8544 (NBS19) and reported on the VPDB scale, by knowing that $\delta^{13}C_{VPDB}$ of RM8544 (NBS19) = 1.95‰. In practice, other reference materials, whose $\delta^{13}C_{VPDB}$ is known, are also used as working standards.

This also demonstrates why the actual isotopic abundance ratio for the VPDB standard, R_{VPDB}, is not normally used in the analysis of isotopic ratios. However, we calibrate the trace gas analyzer for the individual $^{12}CO_2$ and $^{13}CO_2$ mixing ratios, and report our results as mixing ratios and fluxes of each isotopomer. Our primary standards are tanks of CO_2 in air supplied and measured by CMDL, which provides calibrations as total CO_2 mixing ratios and isotope ratios relative to VPDB. Therefore we use R_{VPDB} in Eqs. (A.3) and (A.4) to convert these values to mixing ratios of each isotopomer. Where we report isotope ratios relative to VPDB, we use this same value for R_{VPDB} in Eqs. (A.1) and (A.2) to convert from mixing ratios of individual isotopomers to total mixing ratio and isotope ratios relative to VPDB. Use of a different value for R_{VPDB}, such as that provided by Craig, would change the values we report for isotopomer mixing ratios and fluxes, but it would not change the values we report for isotope ratios.

References

Bevington, P.R., 1969. Data Reduction and Error Analysis for the Physical Sciences. McGraw-Hill, New York.

Bowling, D.R., Baldocchi, D., Monson, R.K., 1999. Dynamics of isotopic exchange of carbon dioxide in a Tennessee deciduous forest. Global Biogeochem. Cycles 13, 903–922.

Bowling, D.R., Tans, P.P., Monson, R.K., 2001. Partitioning net ecosystem CO_2 exchange with isotopic fluxes of CO_2. Global Change Biol. 7, 127–145.

Bowling, D.R., Pataki, D.E., Ehleringer, J.R., 2003a. Critical evaluation of micrometeorological methods for measuring ecosystem–atmosphere isotopic exchange of CO_2. Agric. For. Meteorol. 116, 159–179.

Bowling, D.R., Sargent, S.D., Tanner, B.D., Ehleringer, J.R., 2003b. Tunable diode laser absorption spectroscopy for ecosystem–atmosphere CO_2 isotopic exchange studies. Agric. For. Meteorol. 118, 1–19.

Buchmann, N., Ehleringer, J.R., 1998. CO_2 concentration profiles, and carbon and oxygen isotopes in C_3 and C_4 crop canopies. Agric. For. Meteorol. 89, 45–58.

Ciais, P., Tans, P.P., White, J.W.C., Trolier, M., Francey, R.J., Berry, J.A., Randall, D.R., Sellers, P., Collatz, J.G., Schimel, D.S., 1995. Partitioning of ocean and land uptake of CO_2 as inferred by $\delta^{13}C$ measurements from NOAA Climate Monitoring and Diagnostics Laboratory Global Air Sampling Network. J. Geophys. Res. 100, 5051–5070.

Coplen, T.B., Kendall, C., Hopple, J., 1983. Comparison of stable isotope reference samples. Nature 302, 236–238.

Coplen, T.B., 1994. Reporting of stable hydrogen, carbon, and oxygen isotopic abundances. Pure Appl. Chem. 66, 273–276.

Coplen, T.B., 1995. New IUPAC guidelines for the reporting of stable hydrogen, carbon, and oxygen isotope-ratio data. J. Res. Natl. Inst. Standards Technol. 100, 285.

Craig, H., 1957. Isotopic standards for carbon and oxygen and correction factors for mass-spectrometric analysis of carbon dioxide. Geochim. Cosmochim. Acta 12, 133–149.

De Bièvre, P., Gallet, M., Holden, N.E., Barnes, I.L., 1984. Isotopic abundances and atomic weights of the elements. J. Phys. Chem. Ref. Data 13, 809–891.

Duranceau, M., Ghashghaie, J., Badeck, F., Deleens, E., Cornic, G., 1999. $\delta^{13}C$ of CO_2 respired in the dark in relation to $\delta^{13}C$ of leaf carbohydrates in *Phaseolus vulgaris* L. under progressive drought. Plant Cell Environ. 22, 515–523.

Ehleringer, J.R., Buchmann, N., Flanagan, L., 2000. Carbon isotope ratios in belowground carbon cycle processes. Ecol. Appl. 10, 412–422.

Ehleringer, J.R., Bowling, D.R., Flanagan, L.B., Fessenden, J., Helliker, B., Martinelli, L.A., Ometto, J.P., 2002. Stable isotopes and carbon cycle processes in forests and grasslands. Plant Biol. 4, 181–189.

Farquhar, G.D., Ehleringer, J.R., Hubick, K.T., 1989. Carbon isotope discrimination and photosynthesis. Ann. Rev. Physiol. Plant Mol. Biol. 40, 503–537.

Flanagan, L.B., Ehleringer, J.R., 1998. Ecosystem–atmosphere CO_2 exchange: interpreting signals of change using stable isotope ratios. Trends Ecol. Evol. 13, 10–14.

Flanagan, L.B., Kubien, D.S., Ehleringer, J.R., 1999. Spatial and temporal variation in the carbon and oxygen stable isotope ratio of respired CO_2 in a boreal forest ecosystem. Tellus B 51, 367–384.

Francey, R.J., Tans, P.P., Alison, C.E., Enting, I.G., White, J.W.C., Trolier, M., 1995. Changes in oceanic and terrestrial carbon uptake since 1982. Nature 373, 326–330.

Fung, I., Field, C.B., Berry, J.A., Thompson, M.V., Randerson, J.T., Malström, C.M., Vitousek, P.M., Collatz, G.J., Sellers, P.J., Randall, D.A., Denning, A.S., Badeck, F., John, J., 1997. Carbon 13 exchanges between the atmosphere and biosphere. Global Biogeochem. Cycles 11, 507–533.

Ghashghaie, J., Duranceau, M., Badeck, F.-W., Cornic, G., Adeline, M.-T., Deleens, E., 2001. $\delta^{13}C$ of CO_2 respired in the dark in relation to $\delta^{13}C$ of leaf metabolites: comparison between *Nicotiana sylvestris* and *Helianthus annuus* under drought. Plant Cell Environ. 24, 505–515.

Griffis, T.J., Rouse, W.R., Waddington, J.M., 2000. Interannual variability in net ecosystem CO_2 exchange at a subarctic fen. Global Biogeochem. Cycles 14, 1109–1121.

Keeling, C.D., 1958. The concentration and isotopic abundances of atmospheric carbon dioxide in rural areas. Geochim. Cosmochim. Acta 13, 322–334.

Lin, G., Ehleringer, J.R., 1997. Carbon isotopic fractionation does not occur during dark respiration in C_3 and C_4 plants. Plant Physiol. 114, 391–394.

Lloyd, J., Kruijt, B., Hollinger, D.Y., Grace, J., Francey, R.J., Wong, S.-C., Kelliher, F.M., Miranda, A.C., Farquhar, G.D., Gash, J.H.C., Vygodskaya, N.N., Wright, I.R., Miranda, H.S., Schulze, E.-D., 1996. Vegetation effects on the isotopic composition of atmospheric CO_2 at local and regional scales: theoretical aspects and a comparison between rain forest in Amazonia and a Boreal forest in Siberia. Aust. J. Plant Physiol. 23, 371–399.

Massman, W.J., Lee, X., 2002. Eddy covariance flux corrections and uncertainties in long-term studies of carbon and energy exchanges. Agric. For. Meteorol. 113, 121–144.

Nier, A.O., 1950. A redetermination of the relative abundances of the isotopes of carbon, nitrogen, oxygen, argon, and potassium. Phys. Rev. 77, 789–792.

Pataki, D.E., Ehleringer, J.R., Flanagan, L.B., Yakir, D., Bowling, D.R., Still, C.J., Buchmann, N., Kaplan, J.O., Berry, J.A., 2003. The application and interpretation of Keeling plots in terrestrial carbon cycle research. Global Biogeochem. Cycles 117, 1022.

Pate, J.S., 2001. Carbon isotope discrimination and plant water-use efficiency. In: Unkovich, M., Pate, J., McNeill, A., Gibbs, D.J. (Eds.), Stable Isotope Techniques in the Study of Biological Processes and Functioning of Ecosystems. Kluwer Academic, Boston.

Reed, W.P., 1992. National Institute of Standards and Technology Report of Investigation Reference Materials, reference numbers 8543 and 8546.

Reicosky, D.C., 1997. Tillage-induced CO_2 emission from soil. Nutrient Cycling in Agroecosystems 49, 273–285.

Schmid, H.P., 2002. Footprint modeling for vegetation atmosphere exchange studies: a review and perspective. Agric. For. Meteorol. 113, 159–183.

Schotanus, P., Nieuwstadt, F.T.M., De Bruin, H.A.R., 1983. Temperature measurement with a sonic anemometer and its application to heat and moisture fluxes. Bound.-Lay. Meteorol. 26, 81–93.

Schuepp, P.H., Leclerc, M.Y., MacPherson, J.I., Desjardins, R.L., 1990. Footprint predictions of scalar fluxes from analytical solutions of the diffusion equation. Bound.-Lay. Meteorol. 50, 355–373.

Wagner-Riddle, C., Thurtell, G.W., King, K.M., Kidd, G.E., Beauchamp, E.G., 1996. Nitrous oxide and carbon dioxide fluxes from bare soil using a micrometeorological approach. J. Environ. Qual. 25, 898–907.

Webb, E.K., Pearman, G.I., Leuning, R., 1980. Corrections of flux measurements for density effects due to heat and water vapour transfer. Quart. J. Meteorol. Soc. 106, 85–100.

Yakir, D., Wang, X.F., 1996. Fluxes of CO_2 and water between terrestrial vegetation and the atmosphere estimated from isotope measurements. Nature 380, 515–517.

Yakir, D., Sternberg, L. da Silveira Lobo, 2000. The use of stable isotopes to study ecosystem gas exchange. Oecologia 123, 297–311.

Zhang, Q.L., Li, W.-J., 1990. A calibrated measurement of the atomic weight of carbon. Chin. Sci. Bull. 35, 290–296.